BJP BRITISH JOURNAL OF PHARMACOLOGY
BPS BRITISH PHARMACOLOGICAL SOCIETY

BJP British Journal of Pharmacology

DOI:10.1111/j.1476-5381.2010.00916.x
www.brjpharmacol.org

RESEARCH PAPER

The calmodulin inhibitor *N*-(6-aminohexyl)-5-chloro-1-naphthalene sulphonamide directly blocks human ether *à*-go-go-related gene potassium channels stably expressed in human embryonic kidney 293 cells

Xiao-Hua Zhang[1,3], Man-Wen Jin[1], Hai-Ying Sun[3], Shetuan Zhang[2] and Gui-Rong Li[3]

[1]*Department of Pharmacology, Tongji Medical College, Huazhong University of Science and Technology, Wuhan, Hubei, China,* [2]*Department of Physiology, Queens University, Kingston, Ontario, Canada and* [3]*Departments of Medicine and Physiology, Li Ka Shing Faculty of Medicine, The University of Hong Kong, Pokfulam, Hong Kong SAR, China*

Correspondence
Dr Gui-Rong Li, L8-01, Laboratory Block, Faculty of Medicine Building, The University of Hong Kong, 21 Sassoon Road, Pokfulam, Hong Kong SAR, China. E-mail: grli@hkucc.hku.hk and Dr Man-Wen Jin, Department of Pharmacology, Tongji Medical College, Huazhong University of Science and Technology, Wuhan, China. Email: mwjin@mails.tjmu.edu.cn

Keywords
W-7; hERG channel; $hK_v1.5$; $hK_{IR2.1}$

Received
24 November 2009
Revised
10 May 2010
Accepted
18 May 2010

BACKGROUND AND PURPOSE

N-(6-aminohexyl)-5-chloro-1-naphthalene sulphonamide (W-7) is a well-known calmodulin inhibitor used to study calmodulin regulation of intracellular Ca^{2+} signalling-related process. Here, we have determined whether W-7 would inhibit human ether à-go-go-related gene (hERG or $K_v11.1$) potassium channels, $hK_v1.5$ channels or $hK_{IR}2.1$ channels expressed in human embryonic kidney (HEK) 293 cells.

EXPERIMENTAL APPROACH

The hERG channel current, $hK_v1.5$ channel current or $hK_{IR}2.1$ channel current was recorded with a whole-cell patch clamp technique.

KEY RESULTS

It was found that the calmodulin inhibitor W-7 blocked hERG, $hK_v1.5$ and $hK_{IR}2.1$ channels. W-7 decreased the hERG current (I_{hERG}) in a concentration-dependent manner (IC_{50}: 3.5 μM), and the inhibition was more significant at depolarization potentials between +10 and +60 mV. The hERG mutations in the S6 region *Y652A* and *F656V*, and in the pore helix *S631A*, had the IC_{50}s of 5.5, 9.8 and 25.4 μM respectively. In addition, the compound inhibited $hK_v1.5$ and $hK_{IR}2.1$ channels with IC_{50}s of 6.5 and 13.4 μM respectively.

CONCLUSION AND IMPLICATIONS

These results indicate that the calmodulin inhibitor W-7 exerts a direct channel-blocking effect on hERG, $hK_v1.5$ and $hK_{IR}2.1$ channels stably expressed in HEK 293 cells. Caution should be taken in the interpretation of calmodulin regulation of ion channels with W-7.

Abbreviations

CaMKII, Ca^{2+}-activated calmodulin-dependent protein kinase II; hEAG, human *ether-à-go-go* gene; hERG, human *ether-à-go-go*-related gene; I_{Kr}, rapidly delayed rectifier K^+ current; W-7, *N*-(6-aminohexyl)-5-chloro-1-naphthalene sulphonamide; W-13, *N*-(4-aminobutyl)-5-chloro-2-naphthalene sulphonamide hydrochloride

Introduction

Calmodulin is a ubiquitous Ca^{2+}-binding protein that plays an important role in Ca^{2+}-signalling pathways of eukaryotic cells (Means *et al*. 1982; Rakhilin *et al*., 2004). The Ca^{2+}-activated calmodulin-dependent protein kinase II (CaMKII) is an important regulator of cardiac ionic currents including L-type Ca^{2+} current ($I_{Ca.L}$) (Dzhura *et al*., 2000; Wu *et al*. 2004) and Na^+ current (I_{Na}) (Deschenes *et al*., 2002; Wagner *et al*., 2006; Maltsev *et al*. 2008), and several types of K^+ currents (Schonherr *et al*., 2000; Colinas *et al*., 2006; Li *et al*. 2006; 2007; Ziechner *et al*. 2006; Qu *et al*. 2007). The inhibition of calmodulin and/or CaMKII is believed to be effective in the treatment of ventricular arrhythmias (Wu *et al*., 1999; Gbadebo *et al*. 2002; Anderson, 2005). *N*-(6-Aminohexyl)-5-chloro-1-naphthalene sulphonamide (W-7) is a commonly used calmodulin inhibitor that blocks access to the activation site (Hait and Lazo, 1986; Osawa *et al*. 1998), and has been reported to effectively suppress ventricular arrhythmias in animal models (Wu *et al*., 1999; Gbadebo *et al*. 2002; Anderson, 2005).

Human *ether-à-go-go*-related gene (hERG or $K_v11.1$) (Alexander *et al*., 2009) encodes the α-subunit of the rapidly delayed rectifier K^+ current (I_{Kr}) which contributes importantly to repolarization of the cardiac action potential in the human heart. Dysfunction of I_{Kr} has been implicated in long QT syndrome that can predispose individuals to lethal arrhythmias. Either inherited mutations of hERG or hERG channel block by a variety of drugs can cause the long QT syndrome (Tseng, 2001; Sanguinetti and Mitcheson, 2005). Therefore, hERG channels have been widely used to examine pro-arrhythmic potential of therapeutic agents during drug development. As human *ether-à-go-go* gene (hEAG) K^+ channels are effectively regulated by calmodulin (Schonherr *et al*. 2000; Ziechner *et al*., 2006), the present study was initially designed to investigate whether calmodulin could regulate hERG channels. However, we found that W-7 directly blocked not only hERG channels, but also $hK_v1.5$ or $hK_{IR}2.1$ channels stably expressed in human embryonic kidney (HEK) 293 cells.

Methods

Cell culture and gene transfection

HEK 293 cell lines (Tang *et al*., 2007; Zhang *et al*. 2008) stably expressing hERG gene ($K_v11.1$, provided by Dr G. Robertson, University of Wisconsin, Madison, WI, USA) (Trudeau *et al*., 1995), *$hK_v1.5$* gene (provided from Dr M Tamkun, Colorado State University, CO, USA) and *$hK_{IR}2.1$* gene (provided by Dr Carol A. Vandenberg, University of California at Santa Barbara, CA, USA) (Raab-Graham *et al*., 1994) were cultured in Dulbecco's modified Eagle's medium (Invitrogen, Hong Kong) containing 400 $\mu g \cdot mL^{-1}$ G418 (Sigma-Aldrich, St Louis, MO, USA) and 10% fetal bovine serum. Cells used for electrophysiology were seeded on glass coverslips.

The mutant hERG genes *Y652A*, *F656V* and *S631A* (Gang and Zhang, 2006; Guo *et al*., 2006) were transiently transfected into HEK 293 cells in a 60 mm Petri dish using 10 μL of Lipofectamine 2000 (Invitrogen, Carlsbad, CA, USA) with 4 μg of hERG mutant cDNA in pCDNA3 vector. After 24–48 h, 20–30% of cells expressed hERG channels were used for pharmacological study.

Solutions

Tyrode solution contained (in mM): NaCl 140, KCl 5.0, $MgCl_2$ 1.0, $CaCl_2$ 1.8, NaH_2PO_4 0.33, HEPES 10.0, glucose 10, and pH adjusted to 7.3 with NaOH. The pipette solution contained (in mM): KCl 20, K-aspartate 110, $MgCl_2$ 1.0, HEPES 10, EGTA 5.0 or BAPTA 5.0 (where specified), and GTP 0.1, Na_2-phosphocreatine 5.0, Mg-ATP 5.0, with pH adjusted to 7.2 with KOH.

Data acquisition and analysis

Cells on coverslips were transferred to an open cell chamber (0.5 mL) mounted on the stage of an inverted microscope (Diaphot, Nikon, Japan) and superfused with Tyrode solution at ~2 $mL \cdot min^{-1}$. Experiments were performed at room temperature (22–23°C). The whole-cell patch clamp technique was used as described previously (Tian *et al*., 2006; Tang *et al*., 2007; Zhang *et al*. 2008). Briefly, borosilicate glass electrodes (1.2 mm OD) were pulled with a Brown–Flaming puller (model P-97, Sutter Instrument Co., Novato, CA, USA) and had tip resistances of 2–3 MΩ when filled with the pipette solution. A 3 M KCl–agar bridge was used as reference electrode. Tip potentials were zeroed before the pipette touched the cell. After a gigaohm seal was obtained, the cell membrane was ruptured by gentle suction to establish whole-cell configuration to record hERG, hKv1.5 or hKir 2.1 channel currents. Liquid junction potentials after membrane rupture between the external and pipette solutions (~10.5 mV) were not corrected for all current recording. The membrane currents were recorded with an EPC-10 amplifier and Pulse software (HEKA, Lambrecht, Germany). Command pulses were generated by a 12-bit digital-to-analog converter controlled by Pulse software. Current signals were low-pass filtered at 5 kHz and sampled at 10 kHz. The data were stored on the hard disk of an IBM computer.

Data are presented as means ± SEM. Non-linear curve fitting was performed using Pulsefit (HEKA) and/or Sigmaplot (SPSS Science, Chicago, IL, USA). Paired and/or unpaired Student's *t*-tests were used to evaluate the statistical significance of differences between two group means. One-way ANOVA followed by Tukey's test was used for multiple groups. Values of $P < 0.05$ were considered to be statistically significant.

Materials

W-7 hydrochloride, from Merck Chemicals (Gibbstown, NJ, USA) was prepared as 30 mM stock solutions in dimethyl sulphoxide, and was diluted in experimental solutions to the final concentrations. Calmodulin was purchased from Boppard (Boppard, RP, Germany). All other chemicals were purchased from Sigma-Aldrich.

Results

Inhibition of hERG channel current by W-7

Figure 1A displays the time-course of hERG tail current ($I_{hERG.tail}$) recorded in a representative HEK 293 cell stably expressing hERG channels with the voltage protocol shown in the inset, using a pipette solution containing 5 mM EGTA. The current was gradually inhibited by application of 3 μM W-7 in bath solution, and the effect was partially reversed by washout for 25 min. Original current traces at corresponding time-points are shown on the right side of the panel.

The effect of W-7 on voltage-dependent I_{hERG} was determined in a typical experiment with the voltage protocol shown in the inset (Figure 1B). The current was markedly inhibited by 3 μM W-7, and the inhibitory effect recovered partially upon drug washout (Figure 1B). Figure 1C illustrates the current–voltage (*I–V*) relationships of $I_{hERG.tail}$ during control and after application of 1, 3 and 10 μM W-7. The current was blocked by W-7 in a concentration-dependent manner. Figure 1D displays the percentage of hERG channel inhibition by W-7 relative to control, showing a voltage-dependent inhibition of hERG channels. The inhibition of $I_{hERG.tail}$ by 1, 3 and 10 μM W-7 was stronger at positive potentials between +10 and +60 mV than that at potentials between –20 and 0 mV ($n = 6$, $P < 0.01$ or $P < 0.05$).

Voltage dependence of hERG channels activation (g/g_{max}) was determined by normalizing $I_{hERG.tail}$ in the absence and presence of 3 μM W-7 (Figure 1E). The g/g_{max} curves were fitted to a Boltzmann distribution to obtain the midpoint ($V_{0.5}$) of activation potential and slope factor. The $V_{0.5}$ of hERG channel activation conductance was negatively shifted by

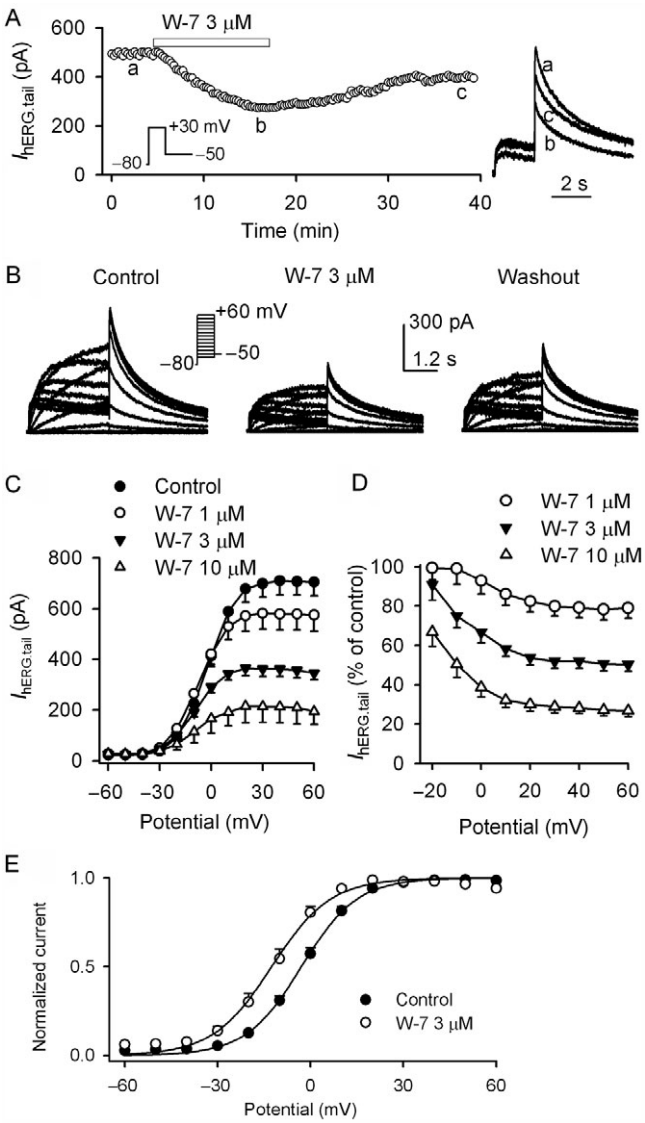

Figure 1

Inhibition of hERG channel current by W-7. (A) Time-course of hERG tail current recorded in a HEK 293 cell stably expressing hERG channels. The current was elicited by a 2 s voltage step to +30 mV from a holding potential of –80 mV, then back to –50 mV (left inset) every 15 s. Original current traces at corresponding time-points are shown in the right of the panel. (B) Voltage-dependent hERG channel currents were recorded in a typical experiment with 5 s voltage steps to between –60 and +60 mV from a holding potential of –80 mV, then back to –50 mV (inset) at 0.05 Hz in the absence and presence of 3 μM W-7. (C) Current–voltage (*I–V*) relationships of $I_{hERG.tail}$ in the absence and presence of 1, 3 and 10 μM W-7. $I_{hERG.tail}$ was measured at the peak of tail current. (D) Voltage dependence of W-7 for inhibiting $I_{hERG.tail}$ ($P < 0.05$ or $P < 0.01$ at potentials of +10 to +50 mV vs. –10 or 0 mV). (E) Voltage dependence of the hERG channel conductance (g/g_{max}) in the absence and presence of 3 μM W-7. The g/g_{max} was determined by normalizing $I_{hERG.tail}$, and fitted to the Boltzmann distribution: $y = 1/\{1 + \exp[(V_m - V_{0.5})/S]\}$, where V_m is the membrane potential, $V_{0.5}$ is the midpoint and S is the slope.

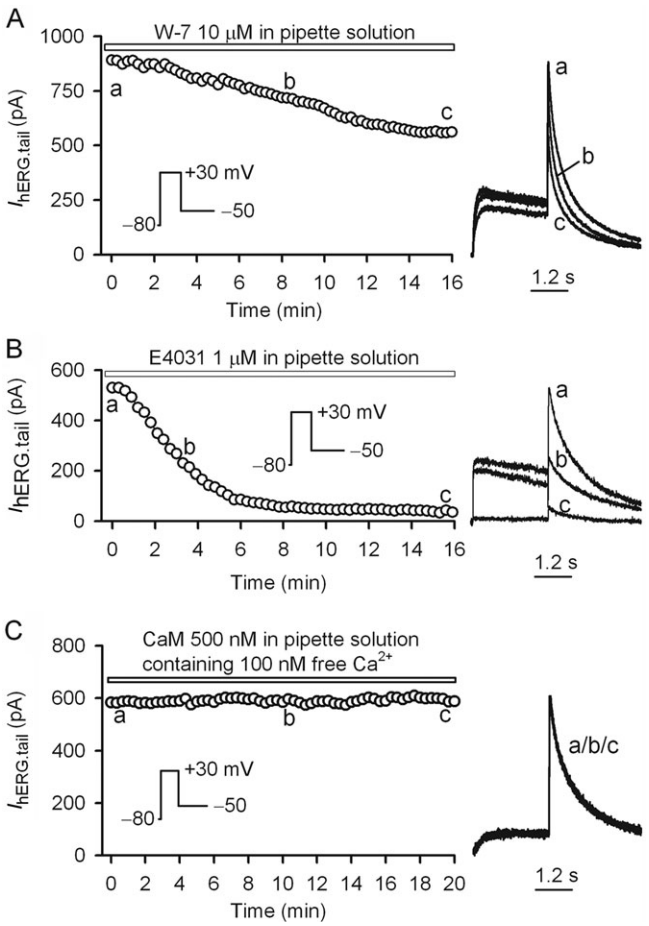

Figure 2

Pipette inclusion of W-7 or calmodulin on hERG channel. (A) Time-course of $I_{hERG.tail}$ recorded with voltage step as shown in the inset in a typical experiment with pipette inclusion of 10 μM W-7 (Rs = 3.4 MΩ), original current traces at corresponding time-points are shown in right of the panel. (B) Time-course of $I_{hERG.tail}$ recorded in a representative cell with pipette inclusion of 1 μM E4031 (Rs = 3.8 MΩ), original current traces at corresponding time-points are shown in right of the panel. (C) Time-course of $I_{hERG.tail}$ recorded with voltage step as shown in the inset in a representative cell with pipette inclusion of 100 nM free Ca^{2+} and 500 nM calmodulin (Rs = 3.6 MΩ), original current traces at corresponding time-points are shown in right of the panel.

9.3 mV (from –5.1 ± 1.3 mV of control to –14.4 ± 1.9 mV, n = 11, P < 0.01) by 3 μM W-7, and no change was observed for the slope factor (8.4 ± 0.3 mV for control, 8.5 ± 0.4 mV for W-7, P = NS).

To determine whether the pipette inclusion of W-7 would show more profound effect on hERG current, 10 μM W-7 was applied in pipette solution. Figure 2A shows that the pipette inclusion of W-7 induced a slow reduction of $I_{hERG.tail}$, and the inhibitory effect was weaker than bath application of W-7. $I_{hERG.tail}$ was decreased by 23 ± 6% (n = 5, P < 0.05 vs. initial membrane rupture) with 10 μM W-7 dialysis for 16 min, while by 71 ± 3% (Figure 1D, n = 7) with 10 μM W-7 application in bath solution for 10 min (P < 0.01 vs. pipette solution application). The pipette inclusion of 10 μM W-7 exhibited 49% less inhibitory effect on hERG channels compared to bath application. To exclude the possibility that the weaker inhibition resulted from the incomplete drug dialysis during the recording period, the hERG channel blocker E4031 (1 μM) was included in pipette solution (Figure 2B). I_{hERG} was gradually inhibited, and steady-state inhibition was observed with 10–12 min dialysis. E4031 inclusion inhibited $I_{hERG.tail}$ by 91.3% (n = 3), indicating that the drug dialysis is complete in HEK 293 cells during the recording period. These results suggest that W-7-induced inhibition of hERG is likely to be related to direct binding to both extracellular and intracellular sites of the channels, because intracellular calmodulin activity is inhibited by the EGTA-buffered pipette solution, in which free Ca^{2+} concentration is close to 0 nM. The experiment with a 5 mM BAPTA-buffered pipette solution showed that W-7 exhibited a similar inhibitory effect on hERG current to that with 5 mM EGTA pipette solution (Supporting Information Figure S1).

To examine whether calmodulin regulated hERG channels, we included 500 nM calmodulin in a 5 mM EGTA pipette solution containing 100 nM free Ca^{2+} (calculated using the Cabuf software created by Dr G. Droogmans in the Department of Physiology, KU Leuven, Leuven, Belgium (ftp://ftp.cc.kuleuven.ac.be/pub/droogmans), which is close to the physiological intracellular free Ca^{2+} level in HEK 293 cells (Tong *et al.*, 1999). Based on Ca^{2+}–calmodulin binding data (Teruel *et al.*, 2000), theoretically about 100 nM calmodulin should be activated. Figure 2C displays the time course of $I_{hERG.tail}$ during a 20 min dialysis of calmodulin after the cell membrane rupture. No significant change in the current was observed in dialysed cells with calmodulin. Similar results were obtained in a total of five cells. In addition, calmodulin inclusion in the pipette solution did not prevent the channel inhibition by W-7 (data not shown). This result indicates that calmodulin may not have the expected effect on hERG channels, consistent with our previous observation that activity of hERG channels is not related to intracellular Ca^{2+} activity (Tang *et al.*, 2007). Therefore, the suppression of the current by W-7 is likely to be due to a direct blocking effect.

W-7 effects on kinetics of inactivation and reactivation of hERG current

The inactivation of hERG channels is believed to play an important role in high-affinity drug binding to hERG channels (Zhang *et al.*, 1999). To examine whether W-7 would affect inactivation time-course

of hERG channels, the current was fully activated and inactivated by a depolarization to +60 mV followed by –100 mV for 10 ms to allow the channels to recover from inactivation, but not enough for channel deactivation (Smith *et al.*, 1996; Spector *et al.*, 1996; Guo *et al.* 2006), and test steps were then applied to different voltages to observe inactivation time-courses before and after 3 μM W-7 (left panel of Figure 3A). The inactivation time constant was obtained by fitting the current decay to a single exponential function. The mean values of voltage-dependent inactivation time constant are illustrated in the right panel of Figure 3A before and after application of 3 μM W-7. W-7 significantly reduced inactivation time constant at voltages from –30 to +40 mV (n = 9, P < 0.05 or P < 0.01 vs. control), which suggests that inactivation of hERG channels is accelerated.

The voltage protocol and recorded currents before and after 3 μM W-7 (left panel of Figure 3B) were used to determine steady-state inactivation (availability) of hERG channels as previously described (Smith *et al.*, 1996; Tang *et al.* 2007). The current curves (right panel of Figure 3B) in the absence (control) and presence of 3 μM W-7 were corrected by extrapolating the exponential decay phase back to the start of the negative voltage step and applying the same relative correction to the initial outward tail current as described previously (Smith *et al.*, 1996; Tang *et al.* 2007). The normalized inactivation curves of corrected I_{hERG} were fitted to a Boltzmann distribution. The half potential ($V_{0.5}$) of hERG channel inactivation was negatively shifted (from –57.5 ± 2.4 mV of control to –67.4 ± 2.7 mV, n = 7, P < 0.01), and the slope factor was slightly, but not significantly, changed from –20.2 ± 0.4 for control to –18.2 ± 0.4 for W-7 (P > 0.05).

The recovery of hERG channels from inactivation was examined before and after 3 μM W-7 application using the standard dual-pulse protocol (left panel of Figure 3C) as previously described (Spector *et al.*, 1996). The rising phase of the current was fitted to a mono-exponential function, and the recovery time constant was plotted against the repolarization potentials (right panel of Figure 3C). The recovery time-constant was significantly reduced by 3 μM W-7 at potentials between –40 and –20 mV (n = 9, P < 0.01 vs. control).

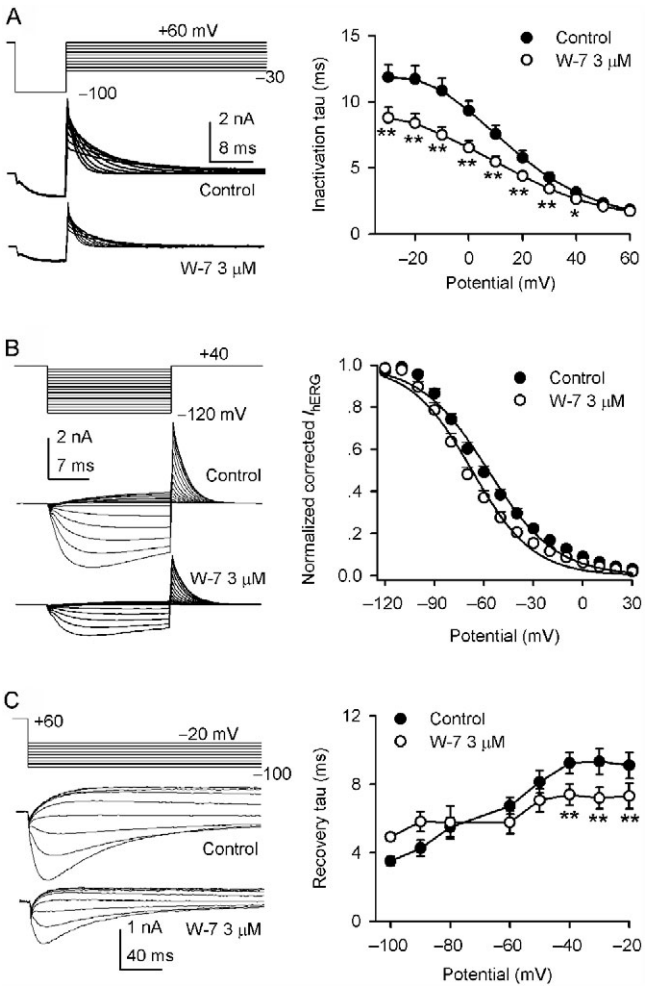

Figure 3

Effects of W-7 on hERG channel kinetics. (A) Left panel, current traces recorded with the protocol were used to evaluate inactivation time-constant of hERG channels. Right panel, mean values of voltage-dependent inactivation time constant (tau) in control and after application of 3 μM W-7 (n = 9, *P < 0.05, **P < 0.01 vs. control). (B) Left panel, current traces obtained with the protocol were used to assess steady-state inactivation. After a 1 s inactivation step to +30 mV, the rapid inactivation of hERG channels was relieved by application of 20 ms test pulses to potentials ranging from –120 to +40 mV. Right panel, steady-state inactivation curves were fitted to a Boltzmann distribution. (C) Left panel, current traces recorded with the protocol were used to evaluate recovery time-constant of hERG channels. The recovery phase of the current was fitted to a mono-exponential function. Right panel, time-constant (tau) of recovery from inactivation was reduced by 3 μM W-7 at voltages from –40 to –20 mV (n = 9, **P < 0.01 vs. control).

Time-dependent block of hERG channels by W-7

The time dependence of development of I_{hERG} block by W-7 was evaluated by holding the potential at –80 mV (upper panel of Figure 4A) to ensure that all hERG channels were in a closed state, followed by a long duration (10 s) voltage step to 0 mV to open the channels. The protocol was applied in control, and discontinued during superfusion of 3 μM W-7 (holding potential –80 mV), then re-applied after 10 min drug exposure. W-7 inhibited I_{hERG} from the beginning of the current activation to end of depolarization step, suggesting that this compound blocked both closed and open channels.

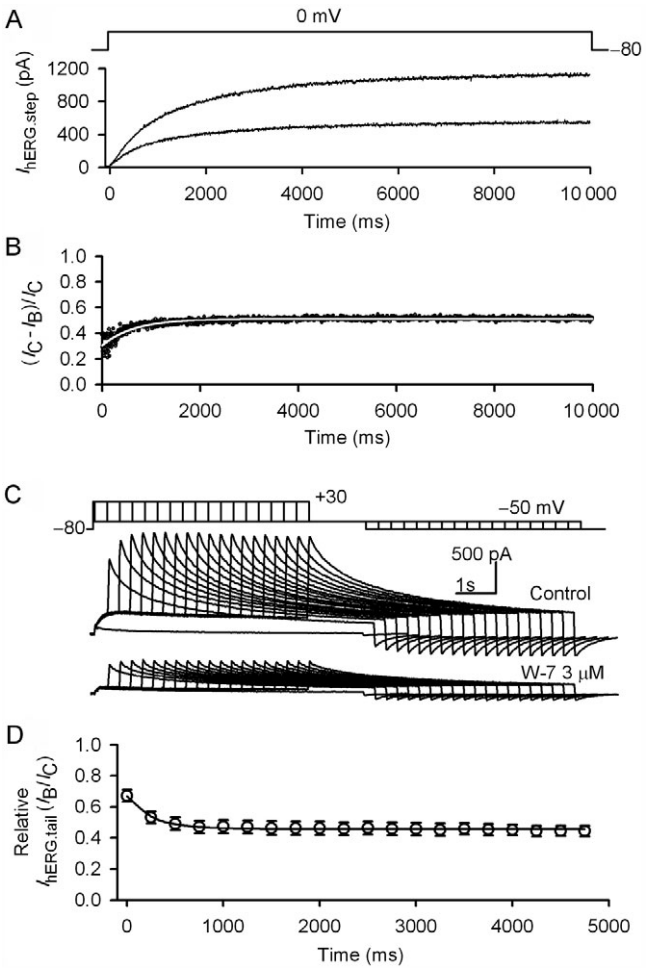

Figure 4

Development of hERG channel block by W-7. (A) Voltage clamp pulse protocol and representative recordings of hERG current before and after exposure of the cell to 3 μM W-7. (B) Drug-sensitive current expressed as a proportion of the current in the absence and presence of 3 μM W-7. Raw data (points) were fitted to a single exponential function with a time-constant of 830 ± 182 ms ($n = 6$). (C) Envelope tail protocol and representative hERG current before (control) and after application of 3 μM W-7. Cells were held at a holding potential of −80 mV and pulsed to depolarizing voltage (+30 mV) for variable durations from 50 to 4950 ms in 250 ms increments. $I_{hERG.tail}$ was recorded upon repolarization to −50 mV. (D) A plot of relative tail current with 3 μM W-7 versus the depolarizing duration. The time-dependent decay in relative tail current was fitted to a single exponential function.

To analyse the contribution of open channel block, onset of channel block was analysed by plotting the time-course of the inhibition by W-7. The onset of open channel block was analysed using the drug-sensitive current formula (Gao *et al.*, 2004): $[(I_C - I_B)/I_C]$, where I_C and I_B are the currents in the absence and presence of W-7 (Figure 4B). The time-constant of the rate of block development was 830.2 ± 182.2 ms ($n = 6$) with 3 μM W-7 ($n = 5$), suggesting W-7 also exerted an open channel blocking effect on hERG channels.

The time-course for the development of W-7 block of hERG channels was further assessed using an envelope of tail test (Tang *et al.*, 2007). Cells were held at a holding potential of –80 mV and pulsed to depolarizing voltage (+30 mV) for variable durations from 50 to 4950 ms in 250 ms increments. $I_{hERG.tail}$ was recorded upon repolarization to –50 mV (upper panel of Figure 4C). The envelope tail test was performed in the same cell before and after addition of 3 μM W-7 (10 min).

The envelope tail current with 3 μM W-7 was expressed relative to control (Figure 4D), and the relative tail current decayed in a pulse duration-dependent manner. The time-course of this decay was fitted to a single exponential function. The onset of hERG channel block by 3 μM W-7 developed rapidly with a time-constant of 328.5 ± 9.9 ms ($n = 5$) at +30 mV.

Tonic block of hERG channel current by W-7 was estimated by the initial value of the relative tail current activated by the envelope protocol. The initial relative tail current at 50 ms with 3 μM W-7 was 67 ± 4% of control, and the steady-state tail current at 4.5 s was 45 ± 4%. Therefore, the fraction of tonic block of hERG channels was about 33% with 3 μM W-7 compared with 23% in open channel block. This result suggests that W-7 blocks hERG channels by binding to both the resting and open states.

Molecular determinants of hERG channel block by W-7

The molecular determinants of W-7 block of hERG channels were investigated using three hERG mutants, *S631A*, *F656V* and *Y652A*. *S631A* is a well-documented pore helix, inactivation-deficient hERG mutant that has been used for investigating the role of inactivation in hERG block (Zhang *et al.*, 1999; Guo *et al.* 2006), and the *Y652* and *F656* are co-located on the S6 transmembrane domain of the hERG channels, both mutations have been shown to attenuate I_{hERG} block by a number of drugs (Zhang *et al.*, 1999; Su *et al.* 2004). To test the molecular determinant of hERG channel block by W-7, the inhibition of *S631A*, *F656V* or *Y652A* channels by this compound was studied in HEK 293 cells transiently expressing these mutants.

Figure 5A illustrates the hERG current traces recorded with a single-voltage protocol as shown in the inset in cells expressing WT hERG, *Y652A*, *F656V* and *S631A* channels, respectively, in the absence and presence of a high concentration of W-7 (30 μM). WT hERG channels were completely blocked by 30 μM W-7, whereas *Y652A* and *F656V*

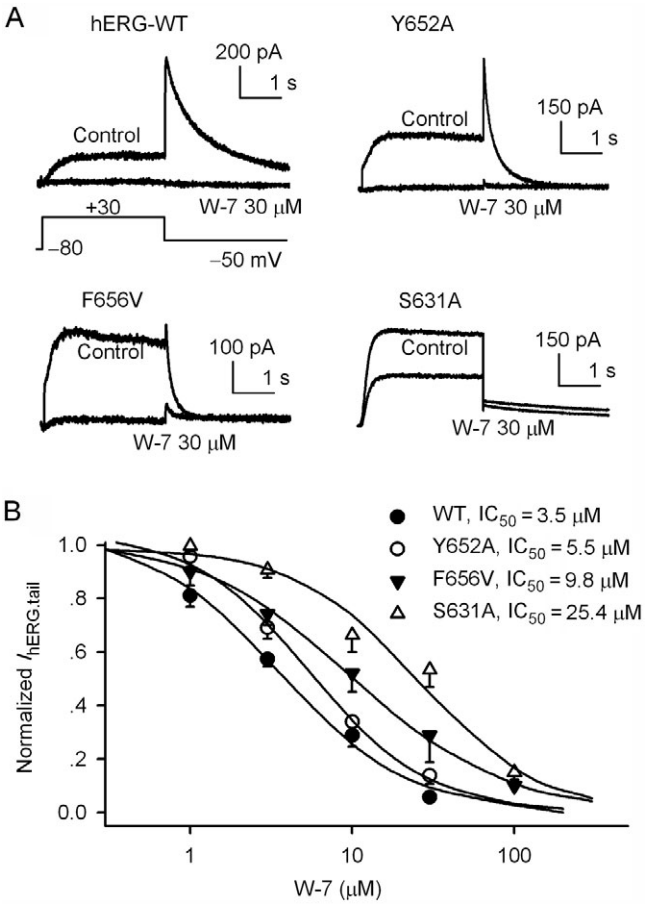

Figure 5

Effects of hERG channel mutations on W-7-induced block. (A) Current traces recorded in the absence (control) and presence of 30 μM W-7 in HEK 293 cells expressing wild-type (WT) or mutant hERG channels: *Y652A*, *F656V* and *S631A* respectively. (B) Concentration–response relationships of W-7 on tail current of WT and various hERG mutant channels were fitted to a Hill equation (n = 4–15 cells for each concentration). The IC_{50} values of W-7 for inhibiting hERG mutants were increased by 1.6- to 7.3-fold, relative to that for WT hERG channels.

channels showed a slight attenuation of I_{hERG} block by W-7. *S631A* was less sensitive to block by 30 μM W-7.

The IC_{50} of W-7 for inhibiting hERG channels was assessed by fitting the concentration–response curves (Figure 5B) to the Hill equation: $E = E_{max}/[1 + (IC_{50}/C)^b]$, where E is the inhibition of current in percentage at concentration C, E_{max} is the maximum inhibition, IC_{50} is the concentration for a half-maximum action and b is the Hill coefficient. The IC_{50} values of W-7 were 3.5, 5.5, 9.8 and 25.4 μM, respectively, for inhibiting the tail current (+30 mV) of WT hERG, *Y652A*, *F656V*, *S631A* mutant channels. These results further demonstrate that W-7 directly binds to hERG channels and blocks the channel.

Inhibition of $hK_v1.5$ channels by W-7

A previous study demonstrated that $hK_v1.5$ was inhibited by the CaMKII inhibitor KN-93 (2-[*N*-(2-hydroxyethyl)]-*N*-(4-methoxybenzenesulphonyl)] amino-*N*-(4-chlorocinnamyl)-*N*-methylbenzylamine) in a CaMKII-independent manner (Rezazadeh *et al.*, 2006). Here, we determined whether the calmodulin inhibitor W-7 could regulate $hK_v1.5$ channels, stably expressed in HEK 293 cells. Figure 6A shows the time-course of $hK_v1.5$ current recorded in a representative cell in the absence and presence of 10 μM W-7. The compound gradually decreased $hK_v1.5$ current, and the effect was partially reversed by drug washout for 30 min. Original current traces at corresponding time-points are shown in right of the panel. Figure 6B displays the effects of W-7 on voltage-dependent $hK_v1.5$ current recorded in a representative cell. W-7 at 10 μM substantially suppressed $hK_v1.5$ current, and the effect was partially reversed by washout (30 min). Figure 6C illustrates the *I–V* relationships of $hK_v1.5$ channels in the absence and presence of 3 and 10 μM W-7. W-7 significantly suppressed activity of $hK_v1.5$ channels at test potentials of 0 to +50 mV ($P < 0.05$ or $P < 0.01$ vs. control). The inhibitory effect of W-7 on $hK_v1.5$ channels, as in hERG channels (Figure 1), exhibited a significant voltage dependence (Figure 6D). Channel block increased with depolarization to more positive potentials. The concentration–response relationship of W-7 is illustrated in Figure 6E, and fitted to the Hill equation. The IC_{50} of W-7 for inhibiting $hK_v1.5$ channels (at +50 mV) was 6.5 μM, and Hill coefficient was 1.1. Moreover, dialysis of cells with 500 nM calmodulin had no effect on $hK_v1.5$ channels (n = 5, data not shown).

Effect of W-7 on $hK_{IR}2.1$ channels

The inward rectifier K^+ current (I_{K1} or $K_{IR}2.1$) was reported to be up-regulated by the inhibition of CaMKII in mice with chronic myocardial CaMKII inhibition resulting from transgenic expression of a CaMKII inhibitory peptide (AC3-I) (Li *et al.*, 2006). Here, we determined whether acute suppression of calmodulin could up-regulate $hK_{IR}2.1$ channels stably expressed in HEK 293 cells. Figure 7A displays the effect of W-7 on $hK_{IR}2.1$ current recorded with the voltage protocol shown in the inset in a representative cell in the absence and presence of 10 μM W-7. W-7 did not increase, instead, suppressed $hK_{IR}2.1$ current, and the inhibitory effect was partially reversed by drug washout (30 min). Figure 7B illustrates the *I–V* relationships of $hK_{IR}2.1$ current before and after application of 3, 10 and 30 μM W-7. The $hK_{IR}2.1$ current was significantly inhibited by W-7 at test potentials of –120 to –80 mV and –60 to –10 mV (n = 6–15, $P < 0.05$ or $P < 0.01$ vs. control)

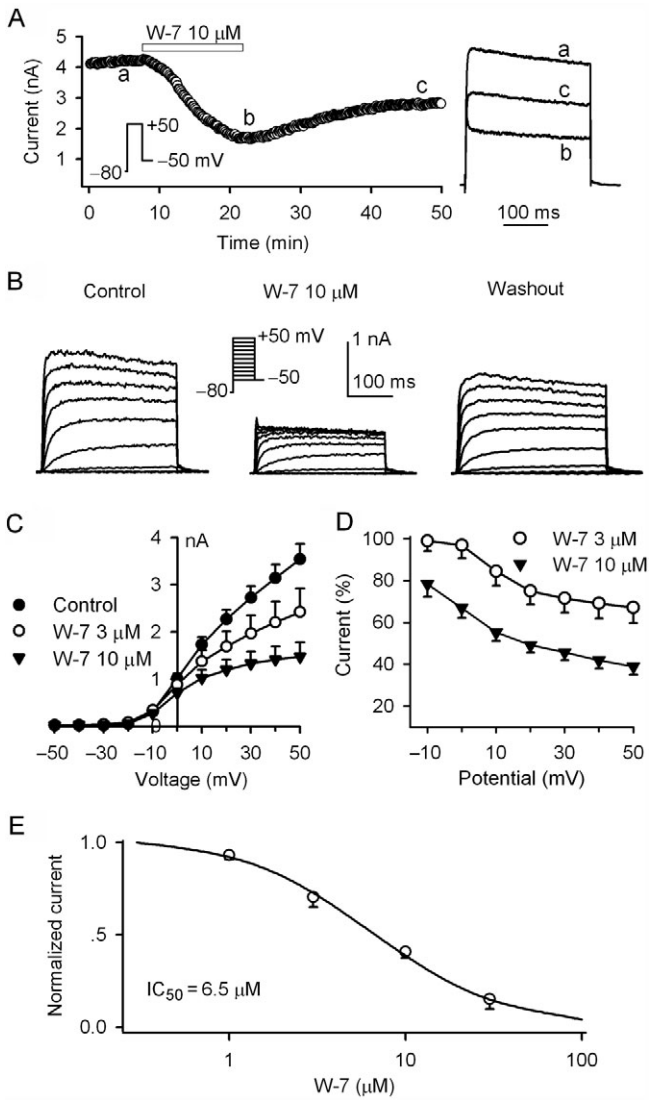

Figure 6

Inhibition of $hK_v1.5$ channels by W-7. (A) Time-course of $hK_v1.5$ current recorded in a HEK 293 cell stably expressing $hK_v1.5$ channels. Membrane current was elicited by a 300 ms voltage step to +50 mV from a holding potential of –80 mV, then back to –50 mV (left insert) every 10 s. Original current traces at corresponding time-points are shown in the right of the panel. (B) Voltage-dependent $hK_v1.5$ current recorded in a representative HEK 293 cell with 300 ms voltage steps to between –50 and +50 mV from a holding potential of –80 mV (inset) at 0.1 Hz in the absence and presence of 10 μM W-7. (C) *I–V* relationships of $hK_v1.5$ (measured at end of the depolarization steps) in the absence and presence of 3 and 10 μM W-7. (D) Voltage dependence of W-7 for inhibiting $hK_v1.5$ channels ($P < 0.05$ or $P < 0.01$ at potentials of +10 to +60 mV vs. –10 or 0 mV). (E) Concentration–response relationship of W-7 for inhibiting $hK_v1.5$ current was fitted to a Hill equation (n = 7–12 cells for each concentration).

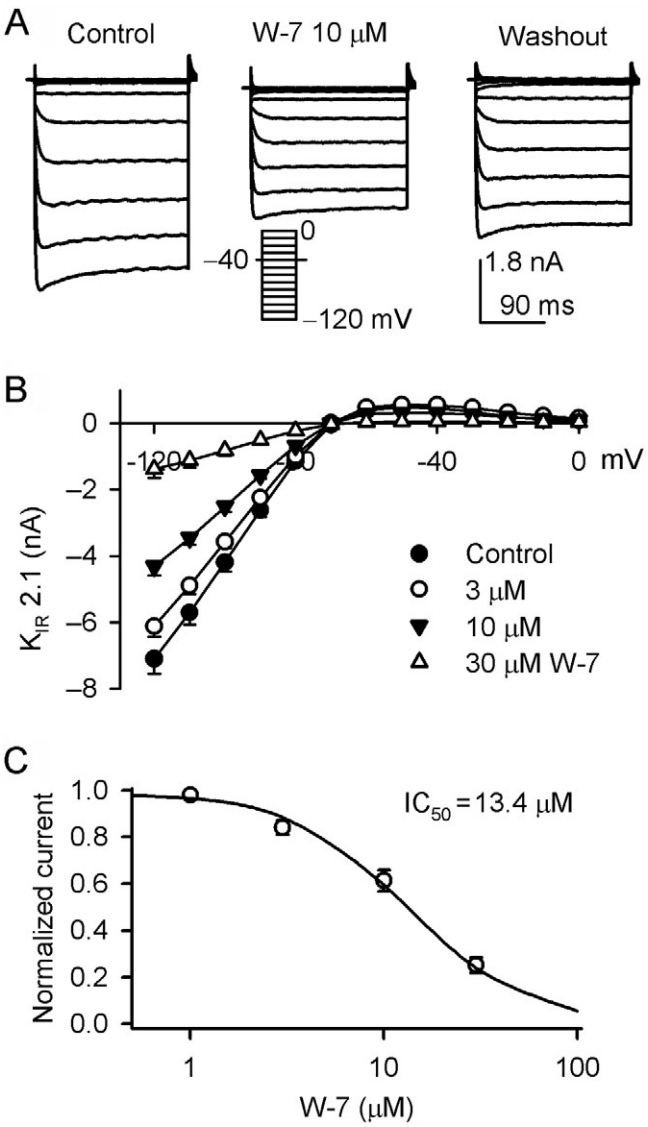

Figure 7

Inhibition of $hK_{IR}2.1$ channels by W-7. (A) Voltage-dependent $hK_{IR}2.1$ current recorded in a representative HEK 293 cell with 200 ms voltage steps to between –120 and 0 mV from a holding potential of –40 mV (inset) at 0.1 Hz in the absence and presence of 10 μM W-7. (B) *I–V* relationships of $hK_{IR}2.1$ current (measured at end of the depolarization steps) in the absence and presence of 3, 10 and 30 μM W-7. (C) The concentration–response relationship of W-7 for inhibiting $hK_{IR}2.1$ current fitted to a Hill equation (n = 5–8 cells for each concentration).

in a concentration-dependent manner. The concentration–response curve (Figure 7C) of W-7 was fitted to a Hill equation. The IC_{50} of W-7 for inhibiting $hK_{IR}2.1$ current (at –120 mV) was 13.4 μM, and Hill coefficient was 1.4. These results indicate that in addition to K_v channel block, W-7 may directly inhibit hK_{IR} channels.

Inhibition of hERG, $hK_v1.5$ and $hK_{IR}2.1$ currents by W-13

N-(4-aminobutyl)-5-chloro-2-naphthalene sulphonamide hydrochloride (W-13) is another membrane-permeable calmodulin inhibitor, with a

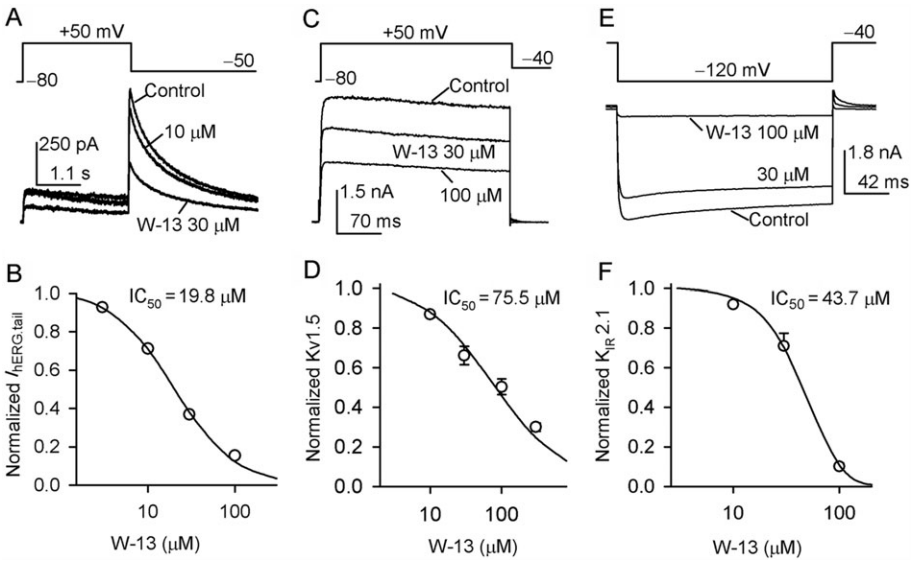

Figure 8

Inhibition of hERG, $hK_v1.5$ and $hK_{IR}2.1$ currents by W-13. (A) hERG current recorded in a representative HEK 293 cell with a 5 s voltage step to +30 mV from a holding potential of −80 mV, then back to −50 mV at 0.02 Hz in the absence and presence of 10 and 30 μM W-13 for 8 min incubation. (B) The concentration–response relationship of W-13 for inhibiting hERG current fitted to a Hill equation (n = 5–9 cells for each concentration). (C) $hK_v1.5$ current recorded in a representative HEK 293 cell with a 300 s voltage step to +50 mV from a holding potential of −80 mV, then back to −40 mV at 0.02 Hz in the absence and presence of 30 and 100 μM W-13. (D) The concentration–response relationship of W-13 for inhibiting $hK_v1.5$ current fitted to a Hill equation (n = 5–7 cells for each concentration). (E) $hK_{IR}2.1$ current recorded in a representative HEK 293 cell with a 200 ms voltage step to −120 mV from a holding potential of −40 mV at 0.02 Hz in the absence and presence of 30 and 100 μM W-13. (F) The concentration–response relationship of W-13 for inhibiting $hK_{IR}2.1$ current fitted to a Hill equation (n = 5–6 cells for each concentration).

different chemical structure from that of W-7, and its effects on hERG, $hK_v1.5$ and $hK_{IR}2.1$ currents were determined. Figure 8 shows that W-13 also suppressed these K^+ currents; however, the inhibitory effect was weaker than W-7. The IC_{50} of W-13 for inhibiting $I_{hERG.tail}$ was 19.8 μM (Hill coefficient, 1.2); 75.5 μM for inhibiting $hK_v1.5$ (Hill coefficient, 0.8), 43.7 μM for inhibiting $hK_{IR}2.1$ currents (Hill coefficient, 2.1).

Discussion

It is believed that increased activity of calmodulin and CaMKII is involved in pathophysiology of different types of cardiac disorders, including ventricular arrhythmias (Anderson, 2005; Lu *et al.*, 2006). Inhibition of calmodulin kinase activity was found to be anti-arrhythmic with the calmodulin inhibitor W-7 (Wu *et al.* 1999; Gbadebo *et al.*, 2002; Anderson, 2005; Lu *et al.*, 2006). It has been recognized that W-7 inhibits calmodulin kinases and regulates additional enzymes (Rakhilin *et al.*, 2004) and/or ion channels including Na^+ channels (Herzog *et al.* 2003; Lee-Kwon *et al.*, 2007), K^+ channels (e.g. $K_v4.3$, $K_v1.3$, KCNQ1/KCNE1) (Chang *et al.* 2001; Shamgar *et al.*, 2006; Qu *et al.*, 2007), pacemaker channels (Rigg *et al.*, 2003; Chatelier *et al.* 2005) and Ca^{2+} channels (Caulfield *et al.* 1991; Anderson *et al.*, 1994; Dzhura *et al.*, 2000; Wu *et al.* 2004) in different types of cells. The effects of W-7 on ion channels were found to be calmodulin dependent for $K_v1.3$ channels in activated human T lymphocytes (Chang *et al.*, 2001), $Na_v1.3$ channels expressed in rat descending vasa recta (Lee-Kwon *et al.*, 2007) and KCNQ1/KCNE1 channels expressed in Chinese hamster ovarian cells or *Xenopus* oocytes (Shamgar *et al.*, 2006), and guinea pig sinus-atrial I_f (Rigg *et al.*, 2003) and ventricular $I_{Ca.L}$ (Anderson *et al.*, 1994; Dzhura *et al.*, 2000; Wu *et al.* 2004). On the other hand, the effects of W-7 were calmodulin independent for rabbit sinus-atrial I_f (Chatelier *et al.*, 2005) and neuronal K^+ currents and Ca^{2+} current (Caulfield *et al.*, 1991). Both calmodulin-dependent and independent effects were also reported for $K_v4.3$ channels expressed in *Xenopus* oocytes (Qu *et al.*, 2007).

The IC_{50} values of W-7 for inhibiting calmodulin-regulated enzymes are variable and tissue dependent in the range of 11–39 μM (Nakajima and Katoh, 1987; Osawa *et al.* 1998). However, no evidence was detected in the present study for calmodulin-dependent processes in tissue-cultured cell lines. We demonstrated that the calmodulin inhibitor W-7 blocked hERG channels stably expressed in HEK 293

cells (Figures 1–5) in a voltage-dependent and concentration-dependent manner (Figure 1). The IC_{50} of W-7 for inhibiting hERG channels was 3.5 μM (Figure 5), 3–11 times less than the IC_{50} values for inhibiting calmodulin-regulated enzymes (Nakajima and Katoh, 1987; Osawa *et al*. 1998). Moreover, another calmodulin inhibitor, W-13, also inhibited hERG channels. These results suggest that hERG channels, unlike hEAG channels (Schonherr *et al*. 2000; Ziechner *et al*., 2006), might not be regulated by calmodulin in HEK 293 cell line. This notion is supported by the following observations: (i) inclusion of W-7 in pipette solution induced a lesser degree of current inhibition than that with bath solution application (Figure 2B); (ii) calmodulin (500 nM) pipette inclusion produced no effect on hERG current (Figure 2B); and (iii) like other hERG channels blockers (Milnes *et al*., 2003; Guo *et al*., 2006; Ridley *et al*., 2006; Su *et al*. 2006; Tang *et al*. 2008), mutations of hERG channels reduced the blocking effect of W-7 (Figure 5).

The blocking properties of hERG channels by W-7 are similar, but not identical, to those of the selective 5-HT re-uptake inhibitor, fluvoxamine, and the metabolite of the aldosterone antagonist spironolactone, canrenoic acid (Caballero *et al*. 2003; Milnes *et al*., 2003). W-7, like fluvoxamine or canrenoic acid (Caballero *et al*. 2003; Milnes *et al*., 2003), blocked hERG channels by binding to both closed and open states of the channel (Figure 4), negatively shifted the activation conductance of the channel and exhibited a voltage-dependent block of the channel (Figure 1C–E). W-7 also negatively shifted the voltage dependence of hERG channel inactivation, and reduced the channel reactivation time-constant at positive potentials (Figure 3), unlike canrenoic acid which had no effect on these parameters (Milnes *et al*., 2003). On the other hand, similar to fluvoxamine, the blocking effect of W-7 was reduced on the mutants in the S6 *Y652A* and *F656V*, and the pore helix mutant *S631A* (Figure 5). Although the changes in onset and recovery of inactivation were statistically significant, these changes were hardly profound. Thus, W-7 unlikely inhibits hERG channel activity through affecting the inactivation gating of the channel.

It is generally recognized that S631 is located at the outer mouth of the pore helix and *S631A* is an inactivation-deficient mutant of hERG channels. The dramatically reduced blocking effect (Figure 5) suggests that the structural changes of *S631A* mutant associated with lack of inactivation may influence W-7 binding to the channel. On the other hand, the mutants *Y652A* and *F656V* exhibited only a slight attenuation of channel block by W-7, suggesting some binding to drug receptor sites within the pore-S6 region, as established in other hERG channel blockers (Milnes *et al*., 2003; Guo *et al*., 2006; Ridley *et al*., 2006; Su *et al*. 2006; Tang *et al*. 2008). The possible contribution of closed-channel blockade to the overall action of W-7 may also be of relevance here. The mutations *F656V*, *Y652A* and *S631A* are anticipated to influence blockade contingent upon channel gating and binding within the pore.

The calmodulin inhibitor W-7 (also W-13), like the CaMKII inhibitor KN-93 (Rezazadeh *et al*., 2006), not only directly suppressed hERG channels, but also inhibited $hK_v1.5$ channels (Figure 6). Moreover, the direct channel block is also applicable to $hK_{IR}2.1$ channels stably expressed in HEK 293 cells (Figure 7). W-7 inhibited $hK_{IR}2.1$ current in a concentration-dependent manner. The IC_{50} values of W-7 for blocking hERG (3.5 μM), $hK_v1.5$ (6.5 μM) and $hK_{IR}2.1$ channels (13.4 μM) were lower than that for inhibiting calmodulin (Osawa *et al*., 1998). However, the possibility that the result from HEK 293 cells may not be identical to that from native cardiac tissue cannot be excluded.

In summary, in addition to the inhibition of $hK_v1.5$ and $hK_{IR}2.1$ channels, the calmodulin inhibitor W-7 directly blocked hERG channels by binding to inactivated and activated states of the channels in a HEK 293 cell line. Therefore, caution should be taken in interpreting observations of calmodulin regulation of ion channels, using W-7.

Acknowledgements

The study was supported in part by Sun Chieh Yeh Heart Foundation of Hong Kong to G-R.L. S.Z. is supported by the Canadian Institutes of Health Research (MOP 84229). The authors thank Dr G. Robertson (University of Wisconsin, Madison, WI, USA) for providing the vector of hERG/pcDNA3; Dr M. Tamkun (Colorado State University, CO, USA) for providing the vector of $hK_v1.5$/pBKCMV; and Dr Carol A. Vandenberg, University of California at Santa Barbara, CA, USA) for providing the vector of $hK_{IR}2.1$ channels.

Conflict of interest

The authors state no conflict of interest.

References

Alexander SPH, Mathie A, Peters JA (2009). *Guide to Receptors and Channels (GRAC)*, 4th edn. Br J Pharmacol 158 (Suppl. 1): S1–S254.

Anderson ME (2005). Calmodulin kinase signaling in heart: an intriguing candidate target for therapy of myocardial dysfunction and arrhythmias. Pharmacol Ther 106: 39–55.

Anderson ME, Braun AP, Schulman H, Premack BA (1994). Multifunctional Ca^{2+}/calmodulin-dependent protein kinase mediates Ca(2+)-induced enhancement of the L-type Ca^{2+} current in rabbit ventricular myocytes. Circ Res 75: 854–861.

Caballero R, Moreno I, Gonzalez T, Arias C, Valenzuela C, Delpon E *et al.* (2003). Spironolactone and its main metabolite, canrenoic acid, block human *ether-a-go-go*-related gene channels. Circulation 107: 889–895.

Caulfield MP, Robbins J, Sim JA, Brown DA, Mac NS, Blackburn GM (1991). The naphthalenesulphonamide calmodulin antagonist W7 and its 5-iodo-1-C8 analogue inhibit potassium and calcium currents in NG108-15 neuroblastoma × glioma cells in a manner possibly unrelated to their antagonism of calmodulin. Neurosci Lett 125: 57–61.

Chang MC, Khanna R, Schlichter LC (2001). Regulation of Kv1.3 channels in activated human T lymphocytes by Ca(2+)-dependent pathways. Cell Physiol Biochem 11: 123–134.

Chatelier A, Renaudon B, Bescond J, El CA, Demion M, Bois P (2005). Calmodulin antagonist W7 directly inhibits f-type current in rabbit sino-atrial cells. Eur J Pharmacol 521: 29–33.

Colinas O, Gallego M, Setien R, Lopez-Lopez JR, Perez-Garcia MT, Casis O (2006). Differential modulation of Kv4.2 and Kv4.3 channels by calmodulin-dependent protein kinase II in rat cardiac myocytes. Am J Physiol Heart Circ Physiol 291: H1978–H1987.

Deschenes I, Neyroud N, DiSilvestre D, Marban E, Yue DT, Tomaselli GF (2002). Isoform-specific modulation of voltage-gated Na(+) channels by calmodulin. Circ Res 90: E49–E57.

Dzhura I, Wu Y, Colbran RJ, Balser JR, Anderson ME (2000). Calmodulin kinase determines calcium-dependent facilitation of L-type calcium channels. Nat Cell Biol 2: 173–177.

Gang H, Zhang S (2006). Na^+ permeation and block of hERG potassium channels. J Gen Physiol 128: 55–71.

Gao Z, Lau CP, Chiu SW, Li GR (2004). Inhibition of ultra-rapid delayed rectifier K^+ current by verapamil in human atrial myocytes. J Mol Cell Cardiol 36: 257–263.

Gbadebo TD, Trimble RW, Khoo MS, Temple J, Roden DM, Anderson ME (2002). Calmodulin inhibitor W-7 unmasks a novel electrocardiographic parameter that predicts initiation of torsade de pointes. Circulation 105: 770–774.

Guo J, Gang H, Zhang S (2006). Molecular determinants of cocaine block of human *ether-a-go-go*-related gene potassium channels. J Pharmacol Exp Ther 317: 865–874.

Hait WN, Lazo JS (1986). Calmodulin: a potential target for cancer chemotherapeutic agents. J Clin Oncol 4: 994–1012.

Herzog RI, Liu C, Waxman SG, Cummins TR (2003). Calmodulin binds to the C terminus of sodium channels Nav1.4 and Nav1.6 and differentially modulates their functional properties. J Neurosci 23: 8261–8270.

Lee-Kwon W, Goo JH, Zhang Z, Silldorff EP, Pallone TL (2007). Vasa recta voltage-gated Na^+ channel Nav1.3 is regulated by calmodulin. Am J Physiol Renal Physiol 292: F404–F414.

Li J, Marionneau C, Zhang R, Shah V, Hell JW, Nerbonne JM *et al.* (2006). Calmodulin kinase II inhibition shortens action potential duration by upregulation of K^+ currents. Circ Res 99: 1092–1099.

Li J, Marionneau C, Koval O, Zingman L, Mohler PJ, Nerbonne JM *et al.* (2007). Calmodulin kinase II inhibition enhances ischemic preconditioning by augmenting ATP-sensitive K^+ current. Channels (Austin) 1: 387–394.

Lu HR, Vlaminckx E, Van de WA, Gallacher DJ (2006). Calmodulin antagonist W-7 prevents sparfloxacin-induced early afterdepolarizations (EADs) in isolated rabbit Purkinje fibers: importance of beat-to-beat instability of the repolarization. J Cardiovasc Electrophysiol 17: 415–422.

Maltsev VA, Reznikov V, Undrovinas NA, Sabbah HN, Undrovinas A (2008). Modulation of late sodium current by Ca^{2+}, calmodulin, and CaMKII in normal and failing dog cardiomyocytes: similarities and differences. Am J Physiol Heart Circ Physiol 294: H1597–H1608.

Means AR, Tash JS, Chafouleas JG (1982). Physiological implications of the presence, distribution, and regulation of calmodulin in eukaryotic cells. Physiol Rev 62: 1–39.

Milnes JT, Crociani O, Arcangeli A, Hancox JC, Witchel HJ (2003). Blockade of HERG potassium currents by fluvoxamine: incomplete attenuation by S6 mutations at F656 or Y652. Br J Pharmacol 139: 887–898.

Nakajima T, Katoh A (1987). Selective calmodulin inhibition toward myosin light chain kinase by a new cerebral circulation improver, Ro 22-4839. Mol Pharmacol 32: 140–146.

Osawa M, Swindells MB, Tanikawa J, Tanaka T, Mase T, Furuya T *et al.* (1998). Solution structure of calmodulin–W-7 complex: the basis of diversity in molecular recognition. J Mol Biol 276: 165–176.

Qu YJ, Bondarenko VE, Xie C, Wang S, Awayda MS, Strauss HC *et al.* (2007). W-7 modulates Kv4.3: pore block and Ca^{2+}-calmodulin inhibition. Am J Physiol Heart Circ Physiol 292: H2364–H2377.

Raab-Graham KF, Radeke CM, Vandenberg CA (1994). Molecular cloning and expression of a human heart inward rectifier potassium channel. Neuroreport 5: 2501–2505.

Rakhilin SV, Olson PA, Nishi A, Starkova NN, Fienberg AA, Nairn AC *et al*. (2004). A network of control mediated by regulator of calcium/calmodulin-dependent signaling. Science 306: 698–701.

Rezazadeh S, Claydon TW, Fedida D (2006). KN-93 (2-[*N*-(2-hydroxyethyl)]-*N*-(4-methoxybenzenesulfonyl)] amino-*N*-(4-chlorocinnamyl)-*N*-methylbenzylamine), a calcium/calmodulin-dependent protein kinase II inhibitor, is a direct extracellular blocker of voltage-gated potassium channels. J Pharmacol Exp Ther 317: 292–299.

Ridley JM, Milnes JT, Hancox JC, Witchel HJ (2006). Clemastine, a conventional antihistamine, is a high potency inhibitor of the HERG K^+ channel. J Mol Cell Cardiol 40: 107–118.

Rigg L, Mattick PA, Heath BM, Terrar DA (2003). Modulation of the hyperpolarization-activated current (I(f)) by calcium and calmodulin in the guinea-pig sino-atrial node. Cardiovasc Res 57: 497–504.

Sanguinetti MC, Mitcheson JS (2005). Predicting drug-hERG channel interactions that cause acquired long QT syndrome. Trends Pharmacol Sci 26: 119–124.

Schonherr R, Lober K, Heinemann SH (2000). Inhibition of human *ether a go-go* potassium channels by Ca(2+)/calmodulin. EMBO J 19: 3263–3271.

Shamgar L, Ma L, Schmitt N, Haitin Y, Peretz A, Wiener R *et al*. (2006). Calmodulin is essential for cardiac IKS channel gating and assembly: impaired function in long-QT mutations. Circ Res 98: 1055–1063.

Smith PL, Baukrowitz T, Yellen G (1996). The inward rectification mechanism of the HERG cardiac potassium channel. Nature 379: 833–836.

Spector PS, Curran ME, Zou A, Keating MT, Sanguinetti MC (1996). Fast inactivation causes rectification of the IKr channel. J Gen Physiol 107: 611–619.

Su Z, Martin R, Cox BF, Gintant G (2004). Mesoridazine: an open-channel blocker of human *ether-a-go-go*-related gene K^+ channel. J Mol Cell Cardiol 36: 151–160.

Su Z, Chen J, Martin RL, McDermott JS, Cox BF, Gopalakrishnan M *et al*. (2006). Block of hERG channel by ziprasidone: biophysical properties and molecular determinants. Biochem Pharmacol 71: 278–286.

Tang Q, Jin MW, Xiang JZ, Dong MQ, Sun HY, Lau CP *et al*. (2007). The membrane permeable calcium chelator BAPTA-AM directly blocks human *ether a-go-go*-related gene potassium channels stably expressed in HEK 293 cells. Biochem Pharmacol 74: 1596–1607.

Tang Q, Li ZQ, Li W, Guo J, Sun HY, Zhang XH *et al*. (2008). The 5-HT(2) antagonist ketanserin is an open channel blocker of human cardiac *ether-a-go-go*-related gene (hERG) potassium channels. Br J Pharmacol 155: 265–273.

Teruel MN, Chen W, Persechini A, Meyer T (2000). Differential codes for free Ca(2+)-calmodulin signals in nucleus and cytosol. Curr Biol 10: 86–94.

Tian M, Dong MQ, Chiu SW, Lau CP, Li GR (2006). Effects of the antifungal antibiotic clotrimazole on human cardiac repolarization potassium currents. Br J Pharmacol 147: 289–297.

Tong J, McCarthy TV, MacLennan DH (1999). Measurement of resting cytosolic Ca^{2+} concentrations and Ca^{2+} store size in HEK-293 cells transfected with malignant hyperthermia or central core disease mutant Ca^{2+} release channels. J Biol Chem 274: 693–702.

Trudeau MC, Warmke JW, Ganetzky B, Robertson GA (1995). HERG, a human inward rectifier in the voltage-gated potassium channel family. Science 269: 92–95.

Tseng GN (2001). I(Kr): the hERG channel. J Mol Cell Cardiol 33: 835–849.

Wagner S, Dybkova N, Rasenack EC, Jacobshagen C, Fabritz L, Kirchhof P *et al*. (2006). Ca^{2+}/calmodulin-dependent protein kinase II regulates cardiac Na^+ channels. J Clin Invest 116: 3127–3138.

Wu Y, Roden DM, Anderson ME (1999). Calmodulin kinase inhibition prevents development of the arrhythmogenic transient inward current. Circ Res 84: 906–912.

Wu Y, Kimbrough JT, Colbran RJ, Anderson ME (2004). Calmodulin kinase is functionally targeted to the action potential plateau for regulation of L-type Ca^{2+} current in rabbit cardiomyocytes. J Physiol 554: 145–155.

Zhang S, Zhou Z, Gong Q, Makielski JC, January CT (1999). Mechanism of block and identification of the verapamil binding domain to HERG potassium channels. Circ Res 84: 989–998.

Zhang DY, Wang Y, Lau CP, Tse HF, Li GR (2008). Both EGFR kinase and Src-related tyrosine kinases regulate human *ether-a-go-go*-related gene potassium channels. Cell Signal 20: 1815–1821.

Ziechner U, Schonherr R, Born AK, Gavrilova-Ruch O, Glaser RW, Malesevic M *et al*. (2006). Inhibition of human ether a go-go potassium channels by Ca^{2+}/calmodulin binding to the cytosolic N- and C-termini. FEBS J 273: 1074–1086.

Supporting information

Additional Supporting Information may be found in the online version of this article:

Figure S1 Inhibitory effect of W-7 on hERG current recorded with a pipette solution containing 5 mM BAPTA. (A) Voltage-dependent hERG channel currents were recorded in a typical experiment with 5 s voltage steps to between –60 and +60 mV from a holding potential of –80 mV, then back to –50 mV (inset) at 0.05 Hz in the absence and presence of 3 μM W-7 for 8 min incubation. W-7 remarkably inhibited hERG current, and the effect is partially

reversed on washout. (B) The concentration–response relationship of W-7 for inhibiting hERG current fitted to a Hill equation (n = 4–6 cells for each concentration). The IC_{50} (at +30 mV) of W-7 for inhibiting hERG tail current was 3.4 μM with a Hill coefficient of 1.1.